https://doi.org/10.48048/tis.2024.7730

Analysis of Hydrodynamic Loads by a Vertical Hollow Cylindrical Structure in A Two-Layer Fluid of Finite Depth

Lham Tashi and Mohammad Hassan*

Department of Mathematics, North Eastern Regional Institute of Science and Technology, Arunachal Pradesh 791109, India

(*Corresponding author's e-mail: mdhassan000@gmail.com)

Received: 17 November 2023, Revised: 18 December 2023, Accepted: 21 December 2023, Published: 30 April 2024

Abstract

This paper aims to study the effect of surge radiation by a vertically hollow cylinder floating in a two-layer fluid of finite depth. Since most of the important characteristics of the oscillating water column are preserved by the hollow cylindrical structure, so the proposed device can be considered as an oscillating water column (OWC) which is one of the important wave energy device. In this two-layer fluid system, the upper layer is bounded above by a free surface and the lower layer is bounded below by a solid impermeable bottom, and the submerged hollow cylindrical structure allows it to oscillate in a surge mode of motion in the upper layer. On the assumption that wave amplitudes are small in comparison to wavelengths, hence the linear water wave theory is applied to formulate boundary value problems by dividing whole domain into 2 sub-domains. The formulated boundary value problems for surge radiated potentials in each sub-domain; we execute to obtain solutions in each sub-domain by using variable separation and matched eigenfunction expansion methods. With the help of obtained surge radiated potentials, we derive the radiation forces by the device in terms of added mass and damping coefficients. A set of influences of different parameters of the device on the added mass and damping coefficients are demonstrated in both surface and internal wave modes of motion. Hydrodynamic coefficients oscillate highly near a particular frequency, which leads to the resonance phenomena. In addition to that, the 3D plots of the free surface elevation in surface and internal wave modes are presented. A density ratio $\gamma = 0.97$ has a higher oscillation than a density ratio $\gamma = 0.93, 0.95$. High oscillations occur around a particular frequency $\omega = 3.83$ due to the resonance phenomenon in which the waves incoming match with the natural motion of the object.

Keywords: Eigen function, Added mass, Damping coefficient, Two-layer fluid, Surge radiation

Introduction

In nature, there is a difference in the density of fluid in oceans due to sea water temperature and salinity of water. It is one of the important reasons to study about the interaction of two-layer fluid with geometrical structure. We consider the pycnocline structure as the two-layer fluid in ocean, where each layer has fixed density and the thin pycnocline separating 2 well mixed fluids. The fluid in each layer is considered to be inviscid and incompressible in nature. Unlike the wave in uniform fluid, the incident waves in a two-layer fluid can propagate with 2 different wavenumbers k_1 and k_2 corresponding to the surface-wave mode and internal-wave mode, respectively. Due to the lower fluid of higher density than the upper fluid, the internal wave modes are generated at the interface as compared to single layer fluid with without internal wave mode. The internal-wave mode has significant effect on the marine structures. A floating structure may undergo 6 degrees of freedom: Three translational and 3 rotational on impact by a wave. Assuming a coordinate system, OXYZ, the 3 translational force are along x, y and z known as surge, sway and heave respectively and 3 rotational along x, y and z as roll, pitch and yaw respectively. The various concept of the interaction of water waves with geometrical structure have been covered [1]. The study on the effect of interaction of waves with floating structures like porous breakwater, very large floating structures (VLFS), have gained popularity [2,3]. Further the installation of wave energy devices on breakwater have gained popularity due to its cost savings and space [4]. There are also works done by researchers in a single layer fluid system to calculate surge and sway forces in [5-7]. Newman [8] investigated negative damping coefficient when calculating hydrodynamic loads on an oscillating ellipsoid in a single layer fluid. Also wave energy devices on breakwater with undulated bottom have been studied [9]. The countries with scarcity of lands and coastal areas have given a great interests on land reclamation through VLFS to build artificial islands, offshore airports, platform for aquatic renewal energy converters,

cages for breeding of marine livestock etc. [13]. Porous body are considered in various marine structures for wave trapping inside the structure. The porous structure dissipates major part of the wave energy to reduce wave transmission to create calm regions in the surrounding of the structure [10-12]. It has seen that no work of the surge radiation of water waves by a vertical hollow cylinder in a two-layer fluid has been done. In this paper, surge radiation of water waves by a vertical hollow cylinder in a two-layer fluid of finite depth is considered.

In oceans, rivers, sea etc. various types of wave energy device are used these days to extract electricity. We use Oscillating water Column (OWC) device which uses a hollow cylinder. OWCs consist of a fixed or floating hollow structure, open to the sea below the water surface that traps air in a chamber above the inner free surface. The wave action alternately compresses and decompresses the trapped air, forcing an air flow moving back and forth through a turbine that drives a generator and produces electricity. This is the reason for considering a hollow cylinder and taking two-layer fluid to mimic the natural environment of a ocean. Here we used method like separation of variables and eigenfunction method. We have calculated added mass and damping coefficients of the radiated waves. Radiation instability was observed by Sturova when a radiation problem of horizontal oscillating cylinder was investigated in a two-layer fluid and she saw negative damping coefficients appearing. Other researchers like Newman and Dolina also observed similar phenomenon [14,15]. The effect of depth ratio and the difference of density on the hydrodynamic coefficients like added mass and damping coefficients is considered in the study. Various parameters like radius of the cylinder and draft of the cylinder is also studied and their effect is presented in graphical form. The results will be useful for the engineers to develop devices using hollow cylindrical structures to extract maximum electrical energy and reduce cost due to inefficient designs and make more efficient devices.

Materials and methods

Formulation

Let us assume that the fluid is inviscid, homogeneous, incompressible, and the motion is an irrotational. The consideration of small-amplitudes enables us to take linear water wave theory. The total depth of the flow is at $z = -h$, and for the upper layer, the fluid depth is h_1 and density is to be ρ_1, and for the lower layer, the depth is h_2 and density is taken to be ρ_2. The draft of the cylinder is at $z = -d$, the bottom is horizontal, and it is impermeable also. The direction of wave propagation is taken into consideration along the x-axis while the y-axis is perpendicular in a right-handed Cartesian coordinate system called $Oxyz$. The origin O is located in the undisturbed free surface.

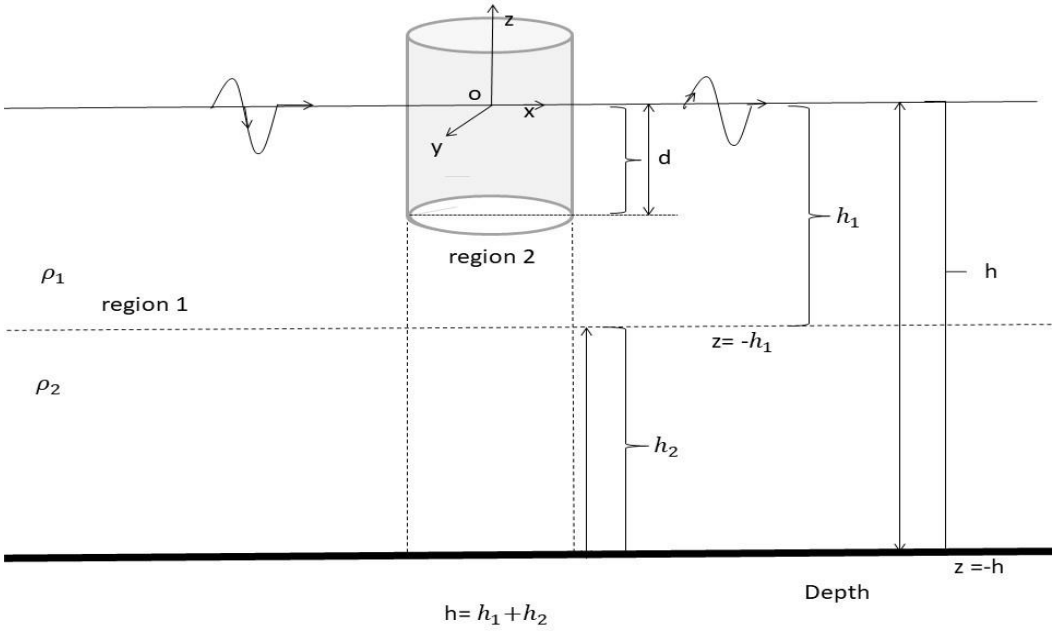

Figure 1 Sketch and definition of the device.

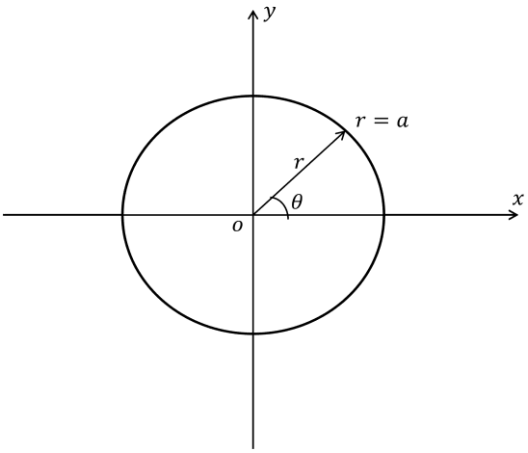

Figure 2 Coordinate system.

As shown in **Figure 1**, In order to seek solution, we divide the whole region into 2 regions: Namely region 1 which is defined by $\Omega_1 = [r\ (\geq a),\ 0 < \theta \leq 2\pi,\ -h \leq z \leq 0]$, and region 2 is defined by $\Omega_2 = [r \leq a,\ 0 < \theta \leq 2\pi,\ -h \leq z \leq 0]$. In these physical regions, we set up the boundary value problems. Let $\Psi_1^{(s)}$, and $\Psi_2^{(s)}$, represent the surge radiated potentials in Ω_1 and Ω_2 respectively. The upper and lower fluid layers are indicated by the superscripts $s = 1, 2$ correspondingly. The flow is considered to be irrotation and periodic with time t. The incident velocity is taken as $\Psi_0^{(s)}(x, y, z, t) = \mathrm{Re}\{\Psi_0^{(s)}(x, y, z)e^{-i\omega t}$. The spatial velocity part $\psi_0{}^{(s)}$ is the incident velocity potential with wavenumber ξ_n and angular frequency ω, propagating along the positive x-direction which is given by:

$$\Psi_0^s = -\frac{i\,\bar{A}(\nu_n)g\,W^{(s)}(\nu_n,\ z)}{\omega}\sum_{m=0}^{\infty}\epsilon_m i^m J_m(\nu_n r)\cos m\theta \tag{1}$$

where $\epsilon_0 = 1$, $\epsilon_m = 2$ for $m \geq 1$, $i = -1$, g is the gravitational acceleration, J (.) is the Bessel function of first kind of order m. It is shown that unlike the homogenous fluid, the wave in a two-layer fluid travels in 2 different wave modes namely surface wave mode and internal wave mode having wavenumbers ν_1 and ν_2, respectively. The wavenumbers ν_n (n = 1, 2) which is determined from the following dispersion relations:

$$\omega^2 = \frac{g\nu\{(t_1+t_2)\pm\sqrt{(t_1+t_2)^2-4\epsilon t_1 t_2(1+\gamma t_1 t_2))}\}}{2(1+\gamma t_1 t_2)}, \tag{2}$$

$\epsilon = 1-\gamma, t_1 = \tanh(\nu h_1), t_2 = \tanh(\nu h_2)$ and:

$$W^{(1)}(\nu_n, z) = \frac{\left(\frac{\omega^2}{g\nu_n}\right)sinh\nu_n z + cosh\nu_n z}{\alpha(\nu_n)}, \tag{3}$$

$$W^{(2)}(\nu_n, z) = \frac{\omega^2}{g\nu_n sinh\nu_n h_2}cosh\,\nu_n(z+h). \tag{4}$$

Here $\bar{A}(\nu_n)$ represents the amplitude defined as:

$$\bar{A}(\nu_n) = b_0^{(1)}(\nu_1)cosh\nu_1 h_1\left(1-\frac{g\nu_1}{\omega^2}tanh\nu_1 h_1\right) \tag{5}$$

$$\bar{A}(\nu_n) = b_0^{(2)}(\nu_2), \tag{6}$$

$$\alpha(\nu_n) = \frac{b_0^{(1)}(\nu_1)}{b_0^{(2)}(\nu_2)}, \tag{7}$$

where $b_0^{(1)}(\nu_1)$ and $b_0^{(2)}(\nu_2)$ represents the amplitudes of the surface and internal wave modes, respectively.

The surface and interface elevations are denoted by $\xi^{(1)}$and $\xi^{(2)}$, respectively. It is given by:

$$\xi^{(s)} = Re\{b_0^s(\nu_n)e^{i(\nu_n x-\omega t)}\} \tag{8}$$

The kinematic and dynamic conditions on the upper surface and the interface satisfied by $\xi^{(1)}$ and $\xi^{(2)}$, are as follows:

$$\Psi_{0,z}^{(1)} - \xi_t^{(1)} = 0; \qquad (z = 0), \tag{9}$$

$$\Psi_{0,t}^{(1)} + g\xi_t^{(1)} = 0; \qquad (z = 0), \tag{10}$$

$$\Psi_{0,z}^{(1)} = \Psi_{0,z}^{(2)} = \xi_t^{(2)}; \qquad (z = -h_1). \tag{11}$$

The governing equation and boundary conditions

The governing equation and related boundary conditions for the radiated potentials in Ω_1 are given by:

$$\boldsymbol{\nabla^2\Psi_1^{(s)} = 0}; \qquad (-\boldsymbol{h < z < 0}, -\infty < \boldsymbol{x, y} < \infty), \tag{12}$$

$$\frac{\boldsymbol{\partial\Psi_1^{(1)}}}{\boldsymbol{\partial z}} = \frac{\boldsymbol{\omega^2}}{\boldsymbol{g}}\boldsymbol{\Psi_1^{(1)}}; \qquad (\boldsymbol{z = 0}) \tag{13}$$

$$\frac{\boldsymbol{\partial\Psi_1^{(2)}}}{\boldsymbol{\partial z}} = \boldsymbol{0}; \qquad (\boldsymbol{z = -h}), \tag{14}$$

$$\frac{\boldsymbol{\partial\Psi_1^{(1)}}}{\boldsymbol{\partial z}} = \frac{\boldsymbol{\partial\Psi_1^{(2)}}}{\boldsymbol{\partial z}}; \qquad (\boldsymbol{z = -h_1}), \tag{14}$$

$$\boldsymbol{\gamma}\left(\frac{\boldsymbol{\partial\Psi_1^{(1)}}}{\boldsymbol{\partial z}} - \frac{\boldsymbol{\omega^2}}{\boldsymbol{g}}\boldsymbol{\Psi_1^{(1)}}\right) = \frac{\boldsymbol{\partial\Psi_1^{(2)}}}{\boldsymbol{\partial z}} - \frac{\boldsymbol{\omega^2}}{\boldsymbol{g}}\boldsymbol{\Psi_1^{(2)}}; \qquad (\boldsymbol{z = -h_1}), \tag{16}$$

and the radiation condition which is valid in the unbounded region:

$$\lim_{r\to\infty}\sqrt{r}\left(\frac{\partial\Psi_1^{(1)}}{\partial r} - ik\Psi_1^{(1)}\right) = 0. \tag{17}$$

The governing equation and the radiated boundary conditions in Ω_2 which are given by:

$$\nabla^2\Psi_2^{(s)} = 0; \qquad (-h < z < 0, -\infty < x, y < \infty,), \tag{18}$$

$$\frac{\partial\Psi_2^{(1)}}{\partial z} = \frac{\omega^2}{g}\Psi_2^{(1)}; \qquad (z = 0), \tag{19}$$

$$\frac{\partial\Psi_2^{(2)}}{\partial z} = 0; \qquad (z = -h), \tag{20}$$

$$\frac{\partial\Psi_2^{(1)}}{\partial z} = \frac{\partial\Psi_2^{(2)}}{\partial z}; \qquad (z = -h_1), \tag{21}$$

$$\gamma\left(\frac{\partial\Psi_2^{(1)}}{\partial z} - \frac{\omega^2}{g}\Psi_2^{(1)}\right) = \frac{\partial\Psi_2^{(2)}}{\partial z} - \frac{\omega^2}{g}\Psi_2^{(2)}; \qquad (z = -h_1), \tag{22}$$

Matching conditions

An analysis of surge velocity potential is carried out to determine the undetermined coefficients which are presented in the obtained surge radiated potential expressions. It is through the maintenance of pressure and velocity continuity along the virtual borders that we intro- duce the necessary matching conditions.

The radiated potential $\boldsymbol{\Psi}$ can be written in the form $\boldsymbol{\Psi^{(s)} = Re\left[\Psi^{(s)}(r,\theta,z)e^{-i\omega t}\right]}$,where the spatial part of the complex velocity potential $\boldsymbol{\Psi^{(s)}}$ is decomposed into 2 potentials defined by:

$$\boldsymbol{\Psi^{(s)} = \begin{cases} \Psi_1^{(s)} & (r \geq a), \\ \Psi_2^{(s)} & (r < a). \end{cases}} \tag{23}$$

at $r = a$, we have:

$$\boldsymbol{\Psi_1^{(s)}(r,\theta,z) = \Psi_2^{(s)}(r,\theta,z); \quad (-h \leq z \leq -d),} \tag{24}$$

$$\boldsymbol{\frac{\partial \Psi_1^{(s)}}{\partial r} = \begin{cases} -i\omega; & (-d \leq z \leq 0), \\ \frac{\partial \Psi_2^{(s)}}{\partial r}; & (-h \leq z \leq -d). \end{cases}} \tag{25}$$

We apply the above appropriate matching conditions along the physical and virtual boundaries between the regions in order to determine the unknown coefficients which are appearing in solutions of the surge radiated velocity potentials.

Results and discussion

Radiated potential

To seek the surge radiated potentials in regions Ω_1 and Ω_2, we need to solve the respective boundary value problems in regions Ω_1 and Ω_2 by using the eigenfunction expansion method and separation of variable technique. Hence, the surge radiated potentials in regions Ω_1 and Ω_2, respectively, are given by:

$$\Psi_1^{(s)}(r,z) = C_0^{(1)}\bar{H}_1(\nu_1,z)W^{(s)}(\nu_1,z) + C_0^{(2)}\bar{H}_1(\nu_2,z)W^{(s)}(\nu_2,z) + \sum_{j=1}^{\infty} C_j^{(1)}\bar{K}_1\left(\nu_j^{*(1)},r\right)W^{(s)}\left(\nu_j^{*(1)},z\right) + \sum_{j=1}^{\infty} C_j^{(2)}\bar{K}_1\left(\nu_j^{*(2)},r\right)W^{(s)}\left(\nu_j^{*(2)},z\right), \tag{26}$$

The eigenfunctions $W^{(1)}(\nu_n,z)$ and $W^{(2)}(\nu_n,z)$ are given by (3) and (4), respectively and $\nu_j^{(1)}$ and $\nu_j^{(2)}$ are roots of the dispersion relations given by:

$$\omega^2 = -\frac{g\nu\{(S_1+S_2)+\sqrt{(S_1+S_2)^2-4\epsilon S_1S_2(1-\gamma S_1S_2)}\}}{2(1-\gamma S_1S_2)}, \tag{27}$$

$$\omega^2 = -\frac{g\nu\{(S_1+S_2)-\sqrt{(S_1+S_2)^2-4\epsilon S_1S_2(1-\gamma S_1S_2)}\}}{2(1-\gamma S_1S_2)}, \tag{28}$$

where:

$$S_1 = tan(\nu h_1), S_2 = tan(\nu h_2), \tag{29}$$

$$\nu_j^{*(1)} = -i\nu_j^{(1)}, \nu_j^{*(2)} = -i\nu_j^{(2)}, \tag{30}$$

$$\bar{H}_1(\nu_n,r) = \frac{H_1^{(1)}(\nu_n r)}{H_1^{(1)}(\nu_n a)}, \tag{31}$$

$$\bar{K}_1\left(\nu_j^{(n)},r\right) = \frac{K_1(\nu_j^{(n)}r)}{K_1(\nu_j^{(n)}a)} \tag{32}$$

where n =1 or 2, $H_1^{(1)}$, is the Hankel functions of first kind order 1 which satisfies the radiation conditions and K_1 is the modified Bessel functions of second kind of order 1 which satisfies the decaying conditions.

$$\Psi_2^{(s)}(r,z) = D_0^{(1)}V_1\left(\eta_0^{(1)},r\right)Y^{(s)}\left(\eta_0^{(1)},z\right) + D_0^{(2)}V_1\left(\eta_0^{(2)},r\right)Y^{(s)}\left(\eta_0^{(2)},z\right) + \left\{ \sum_{k=1}^{\infty} D_k^{(1)}V_1\left(\eta_k^{(1)},r\right)Y^{(s)}\left(\eta_k^{(1)},z\right) + \sum_{k=1}^{\infty} D_k^{(2)}V_1\left(\eta_k^{(2)},r\right)Y^{(s)}\left(\eta_k^{(2)},z\right) \right\} \tag{33}$$

where $V_1(\eta_0^{(1)}, r), V_1(\eta_0^{(2)}, r), V_1(\eta_k^{(1)}, r)$ and $V_1(\eta_k^{(2)}, r)$ are the radial eigenfunctions given respectively by:

$$V_1(\eta_0^{(1)}, r) = \frac{J_1(\eta_0^{(1)} r)}{J_1(\eta_0^{(1)} a)}, \tag{34}$$

$$V_1(\eta_0^{(2)}, r) = \frac{J_1(\eta_0^{(2)} r)}{J_1(\eta_0^{(2)} a)}, \tag{35}$$

$$V_1(\eta_k^{(1)}, r) = \frac{I_1(\eta_k^{(1)} r)}{I_1(\eta_k^{(1)} a)}, \tag{36}$$

$$V_1(\eta_k^{(2)}, r) = \frac{I_1(\eta_k^{(2)} r)}{I_1(\eta_k^{(2)} a)}, \tag{37}$$

The vertical eigenfunctions $Y^{(s)}(\eta_0^{(1)}, z), Y^{(s)}(\eta_0^{(2)}, z), Y^{(s)}(\eta_k^{(1)}, z)$ and $Y^{(s)}(\eta_k^{(2)}, z)$ $k \geq 1$ can be expressed as:

$$Y^{(s)}(\eta_0^{(1)}, z) = \begin{cases} \frac{\eta_0^{(1)} cosh\ \eta_0^{(1)} z + K sinh\, \eta_0^{(1)} z}{K cosh\, \eta_0^{(1)} h_1 - \eta_0^{(1)} sinh\, \eta_0^{(1)} h_1}; & (s = 1, -h_1 \leq z \leq 0) \\ \frac{cosh\, \eta_0^{(1)} (z+h)}{sinh\, \eta_0^{(1)} h_2}; & (s = 1, -h_1 \leq z \leq 0) \end{cases} \tag{38}$$

$$Y^{(s)}(\eta_k^{(1)}, z) = \begin{cases} \frac{\eta_k^{(1)} cos \eta_k^{(1)} z + K sin \eta_k^{(1)} z}{K cos \eta_k^{(1)} h_1 - \eta_k^{(1)} sin\, \eta_k^{(1)} h_1}; & (s = 1, -h_1 \leq z \leq 0) \\ \frac{cos\, \eta_k^{(1)} (z+h)}{sin\, \eta_k^{(1)} h_2}; & (s = 2, -h \leq z \leq -h_1) \end{cases} \tag{39}$$

$$Y^{(s)}(\eta_0^{(2)}, z) = \begin{cases} \frac{\eta_0^{(2)} cosh\ \eta_0^{(2)} z + K sinh\, \eta_0^{(2)} z}{K cosh\, \eta_0^{(2)} h_1 - \eta_0^{(2)} sinh\, \eta_0^{(2)} h_1}; & (s = 1, -h_1 \leq z \leq 0) \\ \frac{cosh\, \eta_0^{(2)} (z+h)}{sinh\, \eta_0^{(2)} h_2}; & (s = 1, -h_1 \leq z \leq 0) \end{cases} \tag{40}$$

$$Y^{(s)}(\eta_k^{(2)}, z) = \begin{cases} \frac{\eta_k^{(2)} cos \eta_k^{(2)} z + K sin \eta_k^{(2)} z}{K cos \eta_k^{(2)} h_1 - \eta_k^{(2)} sin\, \eta_k^{(2)} h_1}; & (s = 1, -h_1 \leq z \leq 0) \\ \frac{cos\, \eta_k^{(2)} (z+h)}{sin\, \eta_k^{(2)} h_2}; & (s = 2, -h \leq z \leq -h_1) \end{cases} \tag{41}$$

Here $\eta_0^{(1)}$ and $\eta_0^{(1)}$ corresponding to surface and internal wave modes are the positive roots of the dispersion relation:

$$\epsilon \eta^2 \bar{t}_1 \bar{t}_2 - \eta K (\bar{t}_1 + \bar{t}_2) + K^2 (1 + \gamma \bar{t}_1 \bar{t}_2) = 0, \tag{42}$$

$\eta_k^{(1)}$ and $\eta_k^{(2)}$ corresponding to surface to surface and internal wave-modes are the roots of the dispersion relation:

$$\epsilon \eta^2 \bar{S}_1 \bar{S}_2 - \eta K (\bar{S}_1 + \bar{S}_2) + K^2 (1 + \gamma \bar{S}_1 \bar{S}_2) = 0, \tag{43}$$

$\bar{t}_1 = \tanh \eta h_1$, $\bar{t}_2 = \tanh \eta h_2$, $\bar{S}_1 = \tan \eta h_1$, $\bar{S}_2 = \tan \eta h_2$ and $K = \frac{\omega^2}{g}$, and $C_0^{(1)}, C_0^{(2)}, C_j^{(1)}, C_j^{(2)}, D_0^{(1)}, D_0^{(2)}, D_k^{(1)}$ and $D_k^{(2)}$, are the unknown coefficients in (26) and (33) which is to be found out by using matching conditions.

Unknown coefficients

To seek the values of undetermined coefficients of surge radiated potentials, one can used matching conditions which conserves the continuity of velocity and pressure of the flow. Subsequently, we apply the radiated potentials (26) and (33) into matching conditions which are given by Eqs. (24) - (25), we get the equations:

$$\sum_{j=0}^{\infty} C_j^{(1)} W^{(s)}\left(\nu_j^{*(1)}, z\right) + \sum_{j=0}^{\infty} C_j^{(2)} W^{(s)}\left(\nu_j^{*(2)}, z\right) = \sum_{k=0}^{\infty} D_k^{(1)} Y^{(s)}\left(\eta_k^{(1)}, z\right) + \sum_{k=0}^{\infty} D_k^{(2)} Y^{(s)}\left(\eta_k^{(2)}, z\right) \tag{44}$$

where:

$$\nu_0^{*(1)} = \nu_0^{(1)} = \nu_1,\ \nu_0^{*(2)} = \nu_0^{(2)} = \nu_2,\ \nu_j^{*(1)} = -i\,\nu_j^{(1)},\ \nu_j^{*(2)} = -i\,\nu_j^{(2)},\ \nu_0^{(1)} C_0^{(1)} \bar{H}_1'\left(\nu_0^{(1)}, a\right) W^{(s)}\left(\nu_0^{(1)}, z\right) + \nu_0^{(2)} C_0^{(2)} \bar{H}_1'\left(\nu_0^{(2)}, a\right) W^{(s)}\left(\nu_0^{(2)}, z\right) \tag{45}$$

$$+ \sum_{j=1}^{\infty} \nu_j^{*(1)} C_j^{(1)} \bar{K}_1'\left(\nu_j^{*(1)}, a\right) W^{(s)}\left(\nu_j^{(1)}, z\right) + \sum_{j=1}^{\infty} \nu_j^{*(2)} C_j^{(2)} \bar{K}_1'\left(\nu_j^{*(2)}, a\right) W^{(s)}\left(\nu_j^{(2)}, z\right) = \begin{cases} -i\omega & (-d \le z \le 0), \\ \sum_{k=0}^{\infty} \eta_k^{(1)} D_k^{(1)} V_1'\left(\eta_k^{(1)}, a\right) Y^{(s)}\left(\eta_k^{(1)}, z\right) + & (-h \le z \le -d). \\ \sum_{k=0}^{\infty} \eta_k^{(2)} D_k^{(2)} V_1'\left(\eta_k^{(2)}, a\right) Y^{(s)}\left(\eta_k^{(2)}, z\right). & \end{cases} \tag{46}$$

Eqs. (44) and (46) are now multiplied by the orthogonal functions in their belonging regions and integrating from $(-h \le z \le 0)$ along the corresponding matching boundary. We obtain the following system of linear equations.

$$-\left\{D_k^{(1)}\right\}_k + \sum_{j=0}^{\infty}\left\{C_j^{(1)}\right\}_j \left[a_{kj}^{(1,1)}\right]_{(k)\times(j)} + \sum_{j=0}^{\infty}\left\{C_j^{(2)}\right\}_j \left[a_{kj}^{(1,2)}\right]_{(k)\times(j)} = 0, \tag{47}$$

$$-\left\{D_k^{(2)}\right\}_k + \sum_{j=0}^{\infty}\left\{C_j^{(1)}\right\}_j \left[a_{kj}^{(2,1)}\right]_{(k)\times(j)} + \sum_{j=0}^{\infty}\left\{C_j^{(2)}\right\}_j \left[a_{kj}^{(2,2)}\right]_{(k)\times(j)} = 0, \tag{48}$$

$$\sum_{k=0}^{\infty}\left\{D_k^{(1)}\right\}_j \left[b_{jk}^{(1,1)}\right]_{(j)\times(k)} + \sum_{k=0}^{\infty}\left\{D_k^{(2)}\right\}_j \left[b_{jk}^{(1,2)}\right]_{(j)\times(k)} - \left\{C_j^{(1)}\right\}_j = \left\{h_j^{(1)}\right\}_j, \tag{49}$$

$$\sum_{k=0}^{\infty}\left\{D_k^{(1)}\right\}_j \left[b_{jk}^{(2,1)}\right]_{(j)\times(k)} + \sum_{k=0}^{\infty}\left\{D_k^{(2)}\right\}_j \left[b_{jk}^{(2,2)}\right]_{(j)\times(k)} - \left\{C_j^{(2)}\right\}_j = \left\{h_j^{(2)}\right\}_j, \tag{50}$$

where:

$$a_{kj}^{(1,1)} = \frac{\int_{-h}^{0} W^{(s)}\left(\nu_j^{(1)}, z\right) Y^{(s)}\left(\eta_k^{(1)}, z\right) dz}{\int_{-h}^{0}\left[Y^{(s)}\left(\eta_k^{(1)}, z\right)\right]^2 dz}, \qquad a_{kj}^{(1,2)} = \frac{\int_{-h}^{0} W^{(s)}\left(\nu_j^{(2)}, z\right) Y^{(s)}\left(\eta_k^{(1)}, z\right) dz}{\int_{-h}^{0}\left[Y^{(s)}\left(\eta_k^{(1)}, z\right)\right]^2 dz}$$
$$a_{kj}^{(2,1)} = \frac{\int_{-h}^{0} W^{(s)}\left(\nu_j^{(1)}, z\right) Y^{(s)}\left(\eta_k^{(2)}, z\right) dz}{\int_{-h}^{0}\left[Y^{(s)}\left(\eta_k^{(2)}, z\right)\right]^2 dz}, \qquad a_{kj}^{(2,2)} = \frac{\int_{-h}^{0} W^{(s)}\left(\nu_j^{(2)}, z\right) Y^{(s)}\left(\eta_k^{(2)}, z\right) dz}{\int_{-h}^{0}\left[Y^{(s)}\left(\eta_k^{(2)}, z\right)\right]^2 dz} \tag{51}$$

$$h_0^{(1)} = -i\omega \frac{\int_{-h}^{0} W^{(s)}\left(\nu_0^{(1)}, z\right) dz}{\nu_0^{(1)} \bar{H}_1'\left(\nu_0^{(1)}, a\right) N_0^{(1)}} \qquad h_0^{(2)} = -i\omega \frac{\int_{-h}^{0} W^{(s)}\left(\nu_0^{(2)}, z\right) dz}{\nu_0^{(2)} \bar{H}_1'\left(\nu_0^{(1)}, a\right) N_0^{(2)}}$$
$$h_j^{(1)} = -i\omega \frac{\int_{-h}^{0} W^{(s)}\left(\nu_j^{(1)}, z\right) dz}{\nu_j^{*(1)} \bar{K}_1'\left(\nu_j^{*(1)}, a\right) N_j^{(1)}} \qquad h_j^{(2)} = -i\omega \frac{\int_{-h}^{0} W^{(s)}\left(\nu_j^{(2)}, z\right) dz}{\nu_j^{*(2)} \bar{K}_1'\left(\nu_j^{*(1)}, a\right) N_j^{(2)}} \tag{52}$$

$$b_{0k}^{(1,1)} = \frac{\eta_k^{(1)} V'\left(\eta_k^{(1)}, a\right) S_{0k}^{(1,1)}}{\nu_0^{(1)} \bar{H}_1'\left(\nu_0^{(1)}, a\right) N_0^{(1)}}, \qquad b_{0k}^{(1,2)} = \frac{\eta_k^{(2)} V'\left(\eta_k^{(2)}, a\right) S_{0k}^{(1,2)}}{\nu_0^{(1)} \bar{H}_1'\left(\nu_0^{(1)}, a\right) N_0^{(1)}},$$
$$b_{0k}^{(2,1)} = \frac{\eta_k^{(1)} V'\left(\eta_k^{(1)}, a\right) S_{0k}^{(2,1)}}{\nu_0^{(2)} \bar{H}_1'\left(\nu_0^{(2)}, a\right) N_0^{(2)}}, \qquad b_{0k}^{(2,2)} = \frac{\eta_k^{(2)} V'\left(\eta_k^{(2)}, a\right) S_{0k}^{(2,2)}}{\nu_0^{(2)} \bar{H}_1'\left(\nu_0^{(2)}, a\right) N_0^{(2)}} \tag{53}$$

$$b_{jk}^{(1,1)} = \frac{\eta_k^{(1)} V'\left(\eta_k^{(1)},a\right) s_{jk}^{(1,1)}}{\nu_j^{*(1)} \bar{K}_1'\left(\nu_j^{*(1)},a\right) N_j^{(1)}}, \qquad b_{jk}^{(1,2)} = \frac{\eta_k^{(2)} V'\left(\eta_k^{(2)},a\right) s_{jk}^{(1,2)}}{\nu_j^{*(1)} \bar{K}_1'\left(\nu_j^{*(1)},a\right) N_j^{(1)}},$$
$$b_{jk}^{(2,1)} = \frac{\eta_k^{(1)} V'\left(\eta_k^{(1)},a\right) s_{jk}^{(2,1)}}{\nu_j^{*(2)} \bar{K}_1'\left(\nu_j^{*(2)},a\right) N_j^{(2)}}, \qquad b_{jk}^{(2,2)} = \frac{\eta_k^{(2)} V'\left(\eta_k^{(2)},a\right) s_{jk}^{(2,2)}}{\nu_j^{*(2)} \bar{K}_1'\left(\nu_j^{*(2)},a\right) N_j^{(2)}} \tag{54}$$

$$N_0^{(n)} = \int_{-h}^{0} \left[W^{(s)}\left(\nu_0^{(n)},z\right)\right]^2 dz, \qquad N_j^{(n)} = \left[W^{(s)}\left(\nu_j^{(n)},z\right)\right]^2 dz, \tag{55}$$

$$S_{0k}^{(1,1)} = \int_{-h}^{-d} \left[Y^{(s)}\left(\eta_k^{(1)},z\right)\right] W^{(s)}\left(\nu_0^{(1)},z\right) dz,$$

$$S_{0k}^{(1,2)} = \int_{-h}^{-d} \left[Y^{(s)}\left(\eta_k^{(2)},z\right)\right] W^{(s)}\left(\nu_0^{(1)},z\right) dz,$$

$$S_{0k}^{(2,1)} = \int_{-h}^{-d} \left[Y^{(s)}\left(\eta_k^{(1)},z\right)\right] W^{(s)}\left(\nu_0^{(2)},z\right) dz,$$

$$S_{0k}^{(2,2)} = \int_{-h}^{-d} \left[Y^{(s)}\left(\eta_k^{(2)},z\right)\right] W^{(s)}\left(\nu_0^{(2)},z\right) dz, \tag{56}$$

$$S_{jk}^{(1,1)} = \int_{-h}^{-d} \left[Y^{(s)}\left(\eta_k^{(1)},z\right)\right] W^{(s)}\left(\nu_j^{(1)},z\right) dz,$$

$$S_{jk}^{(1,2)} = \int_{-h}^{-d} \left[Y^{(s)}\left(\eta_k^{(2)},z\right)\right] W^{(s)}\left(\nu_j^{(1)},z\right) dz,$$

$$S_{jk}^{(2,1)} = \int_{-h}^{-d} \left[Y^{(s)}\left(\eta_k^{(1)},z\right)\right] W^{(s)}\left(\nu_j^{(2)},z\right) dz,$$

$$S_{jk}^{(2,2)} = \int_{-h}^{-d} \left[Y^{(s)}\left(\eta_k^{(2)},z\right)\right] W^{(s)}\left(\nu_j^{(2)},z\right) dz, \tag{57}$$

The unknown coefficients $C_j^{(1)}, C_j^{(2)}, D_k^{(1)}$ and $D_k^{(2)}$ can be obtained by solving Eqs. (47) - (50). To solve this infinite system of linear equations, we need to truncate the infinite series approximately by taking j = 0, 1, 2, 3...J and k = 0, 1, 2, 3...K. Consequently, we obtain a linear system of algebraic equations of order $[2(J+1)+2(K+1)] \times [2(J+1)+2(K+1)]$ and can be solved using MATLAB programming.

Added mass and damping coefficient

The added mass μ_{11} and damping coefficient λ_{11} of the surge radiated potential is calculated by using the formula:

$$\mu_{11} + \frac{i\lambda_{11}}{\omega} = a\omega \int_{-d}^{0} \int_{0}^{2\pi} \rho(z) \Psi_1^{(s)}(a,z)(-\cos^2\theta)\, d\theta \tag{58}$$

The added mass and damping coefficient have been non-dimensionalized by $a\pi\rho_1 h^2$ and $a\pi\omega\rho_1 h^2$, respectively, and the frequency ω by $\sqrt{h/g}$, and $\rho(z)$ is the density in the region defined by:

$$\rho(z) = \begin{cases} \rho_1, & -h_1 \le z \le 0 \\ \rho_2, & -h \le z \le -h_1. \end{cases} \tag{59}$$

Free-surface and interface elevation

The free surface and interface elevation in the region 1, i.e., Δ_1 due to the surge radiated waves in surface and internal wave modes can be calculated by using Eqs. (9) and (11).

$$\xi^{(1)} = Re\left[\frac{\bar{A}(\nu_n)g}{\omega^2}\, icos\theta\Big\{ C_0^{(1)} \bar{H}_1(\nu_1,r) W'^{(1)}(\nu_1,0) + C_0^{(2)} \bar{H}_1(\nu_2,r) W'^{(1)}(\nu_2,0) + \right.$$
$$\left. \sum_{j=1}^{\infty} C_j^{(1)} \bar{K}_1\left(\nu_j^{*(1)},r\right) W'^{(1)}\left(\nu_j^{(1)},0\right) + \sum_{j=1}^{\infty} C_j^{(2)} \bar{K}_1\left(\nu_j^{*(2)},r\right) W'^{(1)}\left(\nu_j^{(2)},0\right) + \Big\} e^{-i\omega t}\right], \tag{60}$$

$$\xi^{(2)} = Re\left[\frac{\bar{A}(\nu_n)g}{\omega^2}\, icos\theta\Big\{ C_0^{(1)}\bar{H}_1(\nu_1,r)W'^{(2)}(\nu_1,-h_1) + C_0^{(2)}\bar{H}_1(\nu_2,r)W'^{(2)}(\nu_2,-h_1) + \sum_{j=1}^{\infty} C_j^{(1)}\bar{K}_1\left(\nu_j^{*(1)},r\right)W'^{(2)}\left(\nu_j^{(1)},-h_1\right) + \sum_{j=1}^{\infty} C_j^{(2)}\bar{K}_1\left(\nu_j^{*(2)},r\right)W'^{(2)}\left(\nu_j^{(2)},-h_1\right) + \Big\}e^{-i\omega t}\right], \quad (61)$$

Numerical results and discussion

On the basis of determined solutions in terms of surge potentials to the radiation problem. The surge radiated potentials enabled us to calculate added mass and damping coefficient of the device. In order to investigate the impact of the device's parameters on the surge radiated potential. It is necessary to compile numerical results in the form of graphical representations along with various values of the parameters, such as draft *d*, radius *a* and depth ratio of the 2 layer fluid $\frac{h_1}{h_2}$. We maintain the following parameter values throughout our calculations in order to plot the numerical outcomes of added mass and damping coefficient: The values of gravitational constant *g* and total depth *h* are taken as $g = 9.8\ m/s^2$, $h = h_1+h_2 = 10\ m$ where *m* represents meter and *s* represents second. The added mass and damping coefficient have been non-dimensionalized by $a\pi\rho_1 h^2$ and $a\pi\omega\rho_1 h^2$ respectively, and the frequency by $\sqrt{h/g}$. For the study of effects of density ratio $\frac{h_1}{h_2}$ on added mass and damping coefficient of a floating cylinder. We have taken (i) $\frac{h_1}{h_2} = \frac{7}{3}$, i.e., the bottom of the cylinder is in the upper layer and (ii) $\frac{h_1}{h_2} = \frac{3}{7}$ i.e. the bottom of the cylinder is in the lower layer. Further, the effect of varying density $\rho\ (z)$ on the added mass and damping coefficient have also been studied. **Figures 3** and **4** demonstrate the non-dimensional added mass and damping coefficient against non- dimensional frequency for different values of radius *a* of the cylinder. We have taken $a = 0.2\ h$, $a = 0.225\ h$ and $a = 0.25\ h$ and the draft of the cylinder is fixed at $d = 0.2\ h$. The depth ratio is kept at $\frac{h_1}{h_2} = \frac{7}{3}$.

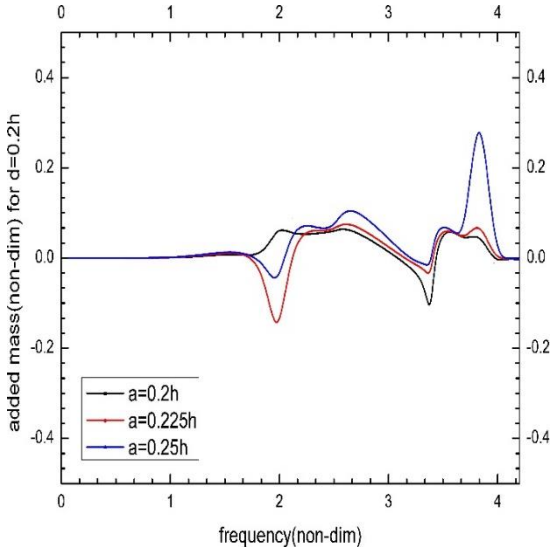

Figure 3 Added mass when we vary the radius *a* of the cylinder and fix γ = 0.97, $d = 0.2\ h$ and $\frac{h_1}{h_2} = \frac{7}{3}$.

From **Figure 3**, we observe that there is no oscillating behavior in lower frequencies but visible oscillations can be seen near the frequency $\omega = 1.98, 3.38,$ and 3.83. It oscillates both positive and negative values in the neighborhood of these frequencies. The high oscillating behavior arises near a particular frequency is due to the resonance phenomenon as the frequency of the incoming waves matches with the natural frequency of the object motion. The wave's frequency diminishes and moves away from natural frequency of the object motion the wave's oscillations decrease and thereby reduced in added mass and damping coefficient. In **Figure 4**, the similar pattern can be seen as that of **Figure 3**. In **Figures 5** and **6**, respectively, the added mass and damping coefficient are demonstrated by varying the draft of the cylinder. We take drafts as $d = 0.2, 0.3, 0.4$ and $0.5\ h$, whereas the radius of the cylinder is taken as $a = 0.2\ h$ and the depth ratio is kept at $\frac{h_1}{h_2} = \frac{7}{3}$. In **Figures 5** and **6**, it is observed that the oscillations near a particular frequency increase with increasing draft of the cylinder. Other than at this particular frequency, the added mass and damping coefficients do not exhibit oscillations. It is due to the resonance

effect that there is such a high fluctuation around a particular frequency.

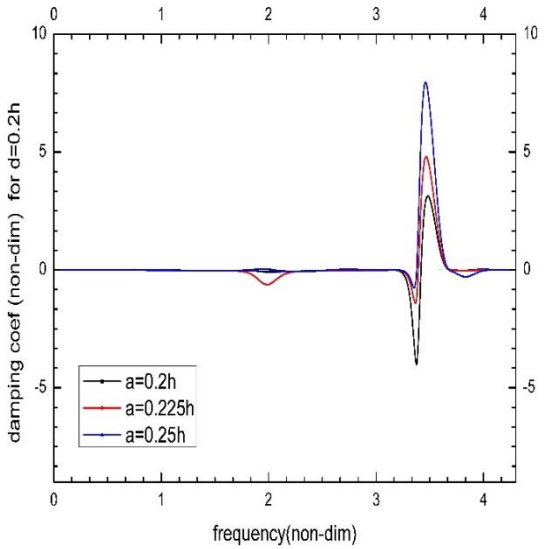

Figure 4 Damping coefficient when we vary the radius a of the cylinder and fix $\gamma = 0.97$, $d = 0.2\ h$ and $\frac{h_1}{h_2} = \frac{7}{3}$.

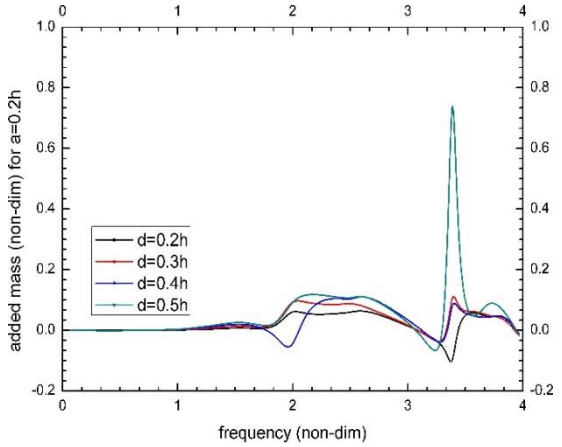

Figure 5 Influence of varying draft d of cylinder on added mass when $\gamma = 0.97$, $a = 0.2$ and $\frac{h_1}{h_2} = \frac{7}{3}$.

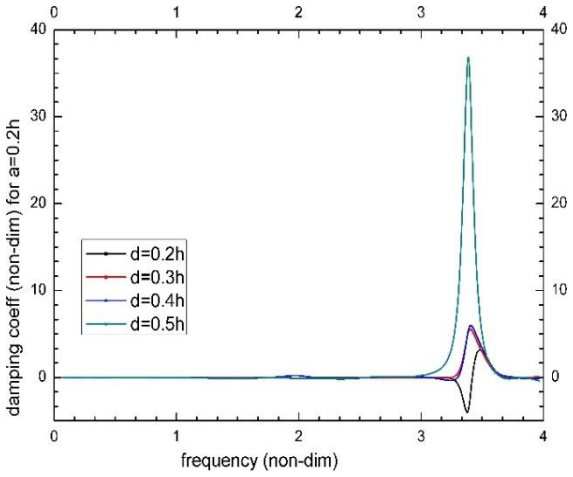

Figure 6 Influence of varying draft d of cylinder on damping coefficient when $\gamma = 0.97$, $a = 0.2\ h$ and $\frac{h_1}{h_2} = \frac{7}{3}$.

Now the results performed for depth ratio $\frac{h_1}{h_2} = \frac{3}{7}$, i.e., the depth of lower layer is larger than the depth of upper layer, **Figures 7** and **8**, respectively, demonstrate the non-dimensional added mass and damping coefficients against non-dimensional frequency for different values of radius of the cylinder. We take $a = 0.2\ h$, $a = 0.225\ h$ and $a = 0.25\ h$. The draft of the cylinder is fixed at $d = 0.2\ h$. In **Figure 7**, we observe that added mass shows no oscillation in lower frequency except $\omega = 3.33$, $\omega = 4.76$ where a very high fluctuation is observed. **Figure 8** shows the almost similar pattern as in **Figure 7**.

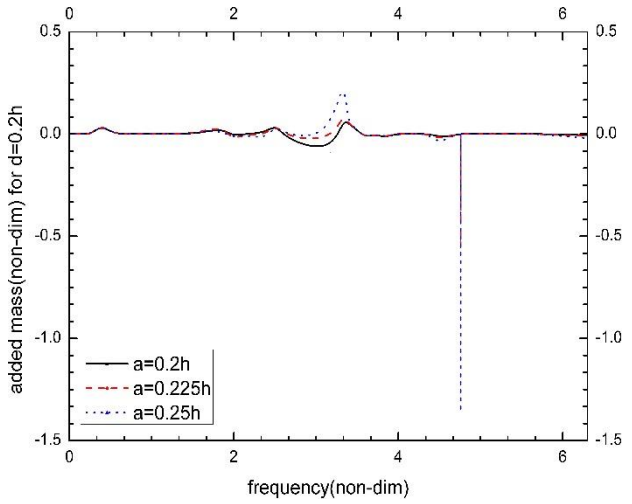

Figure 7 Added mass when we vary the radius a of the cylinder and fix $\gamma = 0.97$, $d = 0.2\ h$ and $\frac{h_1}{h_2} = \frac{3}{7}$.

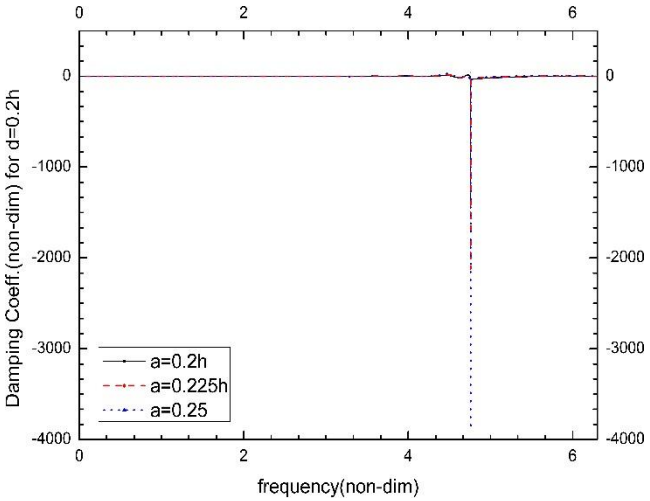

Figure 8 Damping coefficient when we vary the radius a of the cylinder and fix $\gamma = 0.97$, $d = 0.2\ h$ and $\frac{h_1}{h_2} = \frac{3}{7}$.

The high fluctuation values of added mass and damping coefficients at $\omega = 4.76$ show that at this particular frequency resonance is occurred. The motion of the cylinder is favored for this frequency and then motion of the cylinder gets damped or reduced at other frequencies. It was found by researchers like Newman [8] that at high velocities of the object, negative damping coefficient occurs due to the conversion of transnational motion (flow) into wave emission and oscillation of the body. Also Sturova [14] found in a two-layer fluid that when a body moves near fluid layer to another, i.e., when there is a density jump, negative damping coefficients occurred.

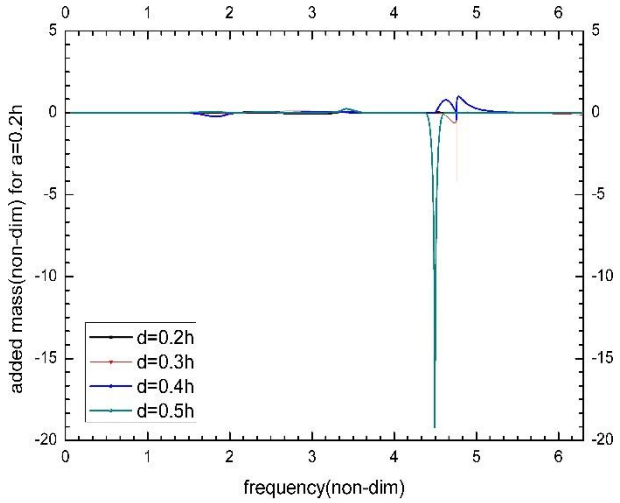

Figure 9 Influence of varying draft d of cylinder on added mass when γ = 0.97, a = 0.2 h and $\frac{h_1}{h_2} = \frac{3}{7}$.

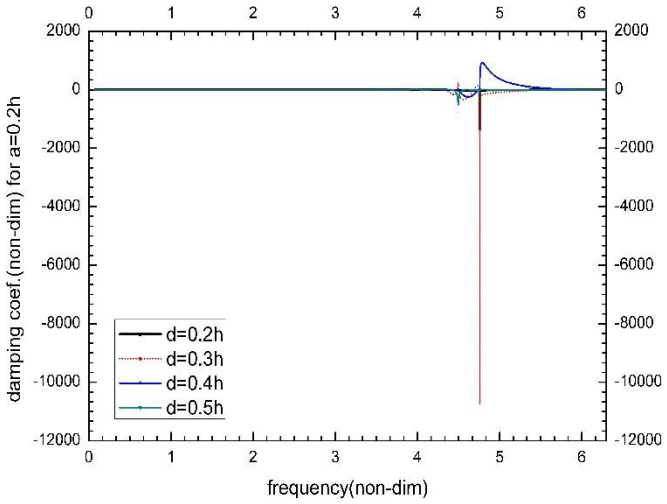

Figure 10 Influence of varying draft d of cylinder on damping coefficient γ = 0.97, a = 0.2 h and $\frac{h_1}{h_2} = \frac{3}{7}$.

Figures 9 and **10** represents the non-dimensionalized added mass and damping coefficient against non-dimensionalized frequency for different values of draft d of the cylinder. We take d = 0.2 h, d = 0.3 h, d = 0.4 h and d = 0.5 h. The radius of the cylinder is fixed at a = 0.2 h.The depth ratio is kept at $\frac{h_1}{h_2} = \frac{3}{7}$. In **Figure 9**, we see the added mass show almost no oscillation on lower frequencies. But we see very high negative fluctuation for the case of d = 0.5 h at ω = 4.49 compared to fluctuation for d = 0.2, 0.3 and 0.4 h. There is a negative fluctuation for the case d = 0.3 h at ω = 4.76. This shows placing the cylinder at the interface of the two-layer fluid experiences a negative fluctuation of added mass.

Figure 10 has similar graph as **Figure 9**. But here there is only one resonance frequency at ω = 4.76. The cylinder placed at the interface, i.e., d = 0.3 h experiences the maximum negative damping coefficient. Thereby motion of the cylinder is favored only at this frequency and at other frequencies, the motion of cylinder gets damped or reduced. Similar explanation as previous case that the cylinder placed at the interface d = 0.3 h with sharp density jump experiences a high negative value of added mass and damping coefficient and at other frequencies, the motion of cylinder gets damped or reduced. Similar explanation as in **Figure 8**, the cylinder placed at the interface d = 0.3 h with sharp density jump experiences a high negative value of added mass and damping coefficient.

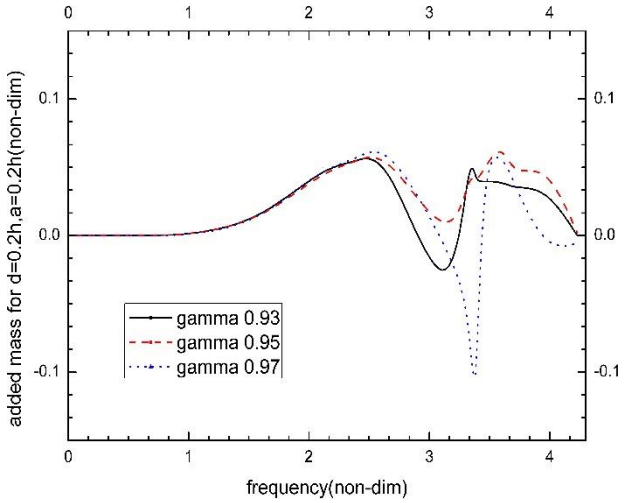

Figure 11 Influence of density ratio of the two- layer fluid on the added mass when $a = 0.2\ h$, $d = 0.2\ h$ and $\frac{h_1}{h_2} = \frac{7}{3}$.

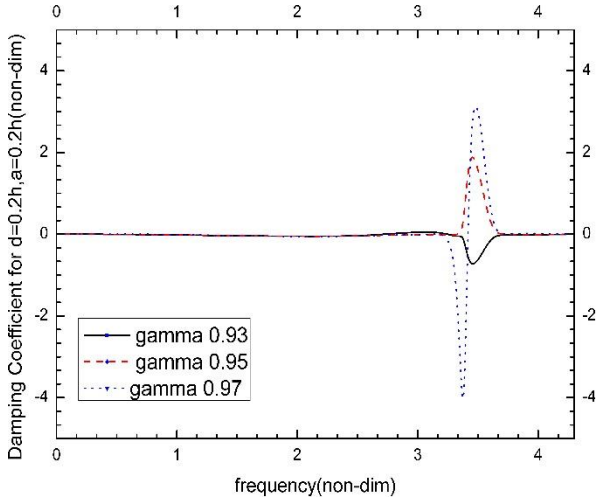

Figure 12 Influence of density ratio of the two- layer fluid on the damping coefficient when $a = 0.2\ h$, $d = 0.2\ h$ and $\frac{h_1}{h_2} = \frac{7}{3}$.

In **Figures 11** and **12**, we study the effect of changing density ratio of the two-layer fluid on the added mass and damping coefficient. Here we fixed draft $d = 0.2\ h$ and the radius as $a = 0.2\ h$. The depth ratio is kept at $\frac{h_1}{h_2} = \frac{7}{3}$.We see in **Figure 11** that the oscillation is occurred for the different density ratios. The oscillation for $\gamma = 0.97$ is greater compared to $\gamma = 0.93$ and $\gamma = 0.95$. In **Figure 12**, we observe no oscillation at lower frequencies. The oscillation only occurs near $\omega = 3.38$. The damping coefficient oscillates for different density ratios in different manner. The density ratio $\gamma = 0.93$ shows only negative oscillation near $\omega = 3.38$ and then at other frequencies, there is no oscillation, the value tend towards zero. For $\gamma = 0.97$ there is both negative and positive oscillations near $\omega = 3.38$ and 3.43 respectively. The density ratio $\gamma = 0.97$ shows the higher oscillation as compared to the density ratio $\gamma = 0.93$ and 0.95.

Figures 13 and **14** give the free surface elevations of a surge radiated wave in surface and internal wave modes. The x, y and z coordinates are non-dimensionalised by dividing with the total depth *h*. From **Figures 13** and **14**, we observe that the free surface elevations have smaller magnitude in the surface wave mode than the internal wave mode.

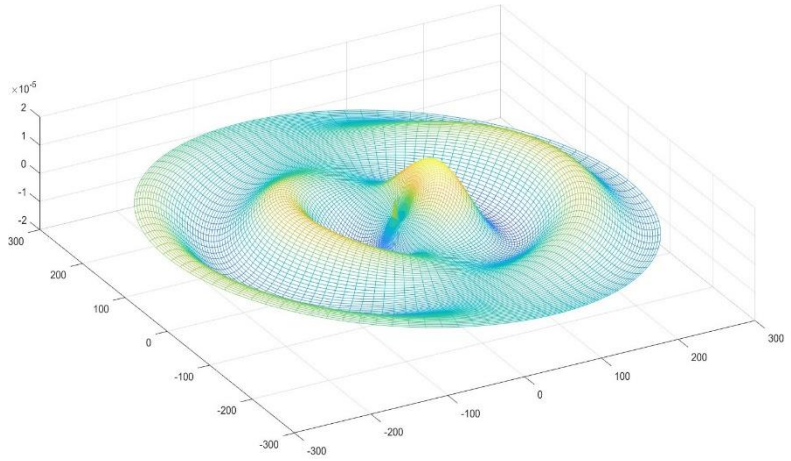

Figure 13 Free surface elevation generated by radiated wave of surface wave mode when γ = 0.97, a = 0.5 h, d = 0.5 h, $\omega\sqrt{h/g} = 0.396$ and $\frac{h_1}{h_2} = \frac{3}{7}$.

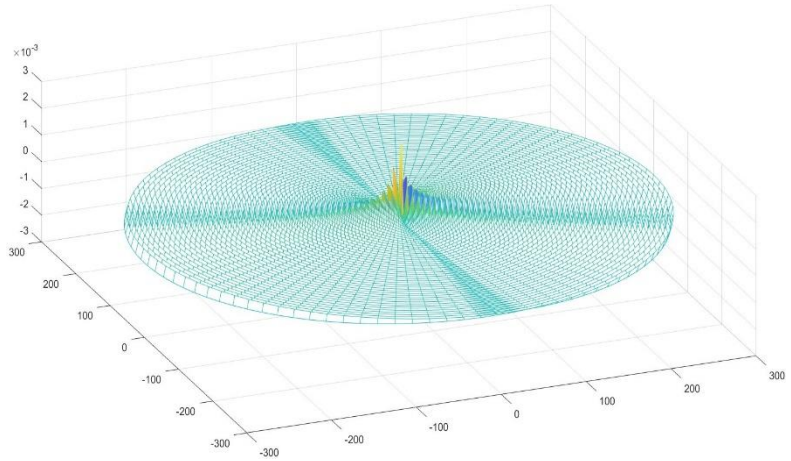

Figure 14 Free surface elevation generated by radiated wave of internal wave mode when γ = 0.97, a = 0.5 h, d = 0.5 h, $\omega\sqrt{h/g} = 0.396$ and $\frac{h_1}{h_2} = \frac{3}{7}$.

Conclusions

In a two-layer fluid system, the wave propagates in two wave modes, namely, surface and the internal wave modes. The surge oscillations of the cylinder generate 2 different modes of radiation waves on the free surface and the internal interface. In this paper, we used the analytic expressions of surge radiated potentials to calculate the added mass and damping coefficient in both surface and internal modes of motion. It is observed that the depth ratio $\frac{h_1}{h_2}$ has small effect on added mass and damping coefficient if the cylinder is placed in the upper layer of the fluid and has a larger effect if the cylinder is in the lower layer of the fluid. The effect is maximum when the cylinder is placed at the interface of the 2 layer. The density ratio of the two-layer fluid also has significant effect on the added mass and damping coefficient. Higher density ratio shows maximum effect on added mass and damping coefficients. As a result, while evaluating the hydrodynamic performance of floating structures, the depth ratio of the 2 layers and the fluid density should be taken into account. At the end, we plot free surface elevations in surface and internal wave modes and it is observed that the free surface elevations of surface mode are smaller than in the internal wave mode.

Acknowledgement

The research scholar shows his gratefulness to North Eastern Regional Institute of Science and Technology, Itanagar, India to carry out research work. The authors are grateful to CSIR, New Delhi, for giving JRF/SRF fellowship during this research work. This work was supported by CSIR as the researcher received CSIR JRF/SRF scholarship from Govt. of India.

References

[1] H Lamb. Hydrodyamics. Cambridge University Press, New York, 1994.
[2] KK Barman, A Chanda and CC Tsai. A mathematical study of a two-layer fluid flow system in the presence of a floating breakwater in front of VLFS. *Appl. Math. Model.* 2023; **122**, 706-30.
[3] KK Barman and SN Bora. Scattering and trapping of water waves by a composite breakwater placed on an elevated bottom in a two-layer fluid flowing over a porous sea-bed. *Appl. Ocean Res.* 2021; **113**, 102544.
[4] K Trivedi and S Koley. Mathematical modeling of breakwater-integrated oscillating water column wave energy converter devices under irregular incident waves. *Renew. Energ.* 2021; **178**, 403-19.
[5] M Biswakarma, P Borah and M Hassan. Added mass and damping coefficients in sway motion for a floating hollow cylinder in a channel of finite width. *Univ. Rev.* 2019; **10**, 201-11.
[6] M Biswakarma, P Borah and M Hassan. Analytical solution of surge hydrodynamic coefficients by an-offshore structure model in a channel of finite width. *J. Comput. Math. Sci.* 2019; **10**, 961-71.
[7] M Hassan, SN Bora and M Biswakarma. Water wave interaction with a pair of floating and submerged coaxial cylinders in uniform water depth. *Mar. Syst. Ocean Tech.* 2020; **15**, 188-98.
[8] JN Newman. The damping of an oscillating ellipsoid near a free surface. *J. Ship Res.* 1961; **5**, 1-19.
[9] S Koley and K Trivedi. Mathematical modeling of oscillating water column wave energy converter devices over the undulated sea bed. *Eng. Anal. Bound. Elem.* 2020; **117**, 26-40.
[10] S Singla, H Behera and SC Martha. Scattering of Obliquely incident water waves by a surface piercing porous box. *Ocean Eng.* 2019; **193**, 106577.
[11] S Singla, H Behera, SC Martha and T Sahoo. Scattering of water waves by very large floating structure in the presence of a porous box. *J. Offshore Mech. Arctic Eng.* 2020; **144**, 041904.
[12] SA Selvan and H Behera. Wave energy dissipation by a floating circular flexible porous membrane in single and two-layer fluids. *Ocean Eng.* 2020; **206**, 107374.
[13] SA Selvan, R Gayathri, H Behera and MH Meylan. Surface wave scattering by multiple flexible fishing cage system. *Phys. Fluid.* 2021; **33**, 037119.
[14] IV Sturova. Radiation instability of a circular cylinder in a uniform flow of a two-layer fluid. *J. Appl. Math. Mech.* 1997; **61**, 957-65.
[15] IS Dolina. *Amplification of the oscillatory motion of a body in a stratified fluid.* Izv. Akad Nauk SSSR. MZhG, Russian, 1984.